



**Acoustics'08  
Paris**  
June 29-July 4, 2008

[www.acoustics08-paris.org](http://www.acoustics08-paris.org)

## Array based measurement of radiated and absorbed sound intensity components

Jørgen Hald<sup>a</sup>, Jakob Mørkholt<sup>a</sup>, Pierre Hardy<sup>b</sup>, Dominique Trentin<sup>b</sup>, Martin Bach-Andersen<sup>c</sup> and Graeme Keith<sup>c</sup>

<sup>a</sup>Brüel & Kjær Sound & Vibration Measurement A/S, Skodsborgvej 307, DK-2850 Nærum, Denmark

<sup>b</sup>Dassault Aviation, 80 quai marcel Dassault - Cédex 300, 92552 Saint Cloud, Cédex, France

<sup>c</sup>Ødegaard & Dannekiold-Samsøe A/S, Titangade 15, DK-2200 København Ø, Denmark  
jhald@bksv.com

In some cases it is important to be able to measure not only the total sound intensity on a source surface, but also the components of that intensity due to sound radiation and due to absorption. The radiated intensity is here defined as the intensity that would be radiated under free-field conditions, while the absorbed intensity is associated with an incident field component. Considering these intensity components on a small section of for example the panels in an aircraft cabin, the distinction between radiated and incident fields is not obvious, because their sources may be close to each other on the same larger panel section. This problem is discussed in the paper, and two different methods for measurement of the two components based on measurements with a dual layer array are introduced: One based on surface absorption coefficient and one based on surface admittance. In both cases two measurements are required: A measurement of surface properties and an operational measurement. The strengths, weaknesses and limitations of the two methods are discussed and investigated through simulated and real measurements.

## 1 Introduction

The present paper is based on work done in the European project CREDO, which deals with noise in aircraft and helicopter cabins. The focus is therefore on radiated and absorbed intensity components on cabin panels. Since the radiated intensity is often seen from the perspective of the cabin, it will be sometimes called Entering Intensity (EI).

Consider the radiation of sound from a small surface segment in a cabin environment. Such a surface segment may radiate sound energy because of external forcing, causing the surface to vibrate, and it may absorb energy from an incident sound field because of finite surface acoustic impedance. When measuring the sound intensity over the surface segment with an intensity probe, the total intensity  $I_{\text{tot}}$  will be measured. Assuming the radiated field and the incident field to be mutually incoherent, the total intensity is equal to the sum of the radiated sound intensity  $I_{\text{rad}}$  that would exist with no incident field and the sound intensity component  $I_{\text{abs}}$  due to absorption from the incident field:

$$I_{\text{tot}} = I_{\text{rad}} + I_{\text{abs}} \quad (1)$$

Here, the radiated intensity will typically be positive, while the component due to absorption will typically be negative, so the total measured intensity may be small although the radiated intensity is relatively high. This happens for vibrating panels with an absorptive surface. Often it is of interest to know not only the total intensity, but also the components due to radiation and absorption. For example, this kind of information is needed in energy based modelling that describes the energy flow between sub-systems, [1].

The assumption of incoherent radiated and incident field components is probably reasonable for Turbulent Boundary Layer (TBL) noise in an aircraft cabin, where there is a huge number of incoherent excitations. A first idea could therefore be to estimate the radiated intensity as the product of total intensity and the coherence with a reference vibration signal measured under the position of the intensity probe. However, with finite surface impedance, the surface velocity and thus the reference signal will contain a component due to the incident field. Also, one reference may not be sufficient to completely represent the radiated field at the measurement position.

The methods to be investigated in the present report are not based on correlation, but on separation of different sound field components via the spatial sound field information provided by an array. The radiated intensity is estimated as

the intensity that would exist, if the incident and scattered field components could be taken away. So a free-field radiation condition is simulated. The idea is to first separate the incident field component, then use measured information about the scattering properties of the panel (geometry and surface admittance or absorption coefficient) to calculate the scattered field, and finally subtract the incident and scattered fields from the total sound field.

## 2 Methodology description

The array measurements will typically be cross-spectral measurements. Separate reference signals could be measured, but because of the large number of independent sources of TBL noise we have chosen to simply measure the full cross spectral matrix between all array microphones, and then derive a Principal Component sound field representation based on that [2]. As a consequence no phase information is available between different array positions, so a separate patch holography calculation has to be performed for each position. We used a Double Layer Array (DLA), and the processing was performed using Statistically Optimized NAH (SONAH), [3-4]. In the following we will consider only a single Principal Component, i.e. a spatially coherent sound field with coherent sources. We shall use a complex time harmonic representation with the time variation  $e^{j\omega t}$  suppressed

### 2.1 Extraction of incident field

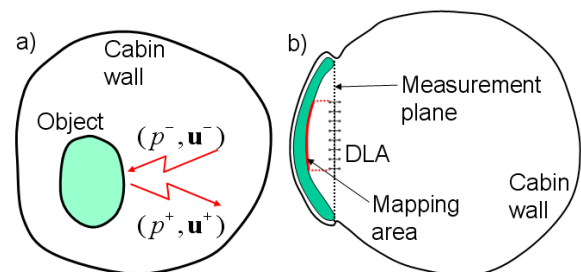


Fig. 1. Separation of inward and outward propagating field components  $(p^-, \mathbf{u}^-)$  and  $(p^+, \mathbf{u}^+)$ : a) Clearly separated sources. b) Smooth transition between sources.

A basic array processing task is that of extracting the incident sound field from the total sound field. Considering the sound field on a small panel segment in an aircraft cabin, the distinction between (sources of) the incident field and (sources of) the radiated field is, however, not obvious, even when we look at the field very near the panel segment. Because of coherent vibration components and significant

mutual radiation impedances between neighbouring panel segment, some neighbouring segments should be included as source of the radiated field. Figure 1 illustrates how this distinction can be made in practice with a DLA. Using SONAH holography on a DLA measurement, the sound field components  $(p^-, \mathbf{u}^-)$  and  $(p^+, \mathbf{u}^+)$  with sources on different sides of the array plane can be separated, [3,4]:

$$(p_{total}, \mathbf{u}_{total}) = (p^-, \mathbf{u}^-) + (p^+, \mathbf{u}^+) \quad (2)$$

The pressure  $p^-$  and the velocity vector  $\mathbf{u}^-$  represent the field incident on the source area of interest, while the outward propagating field component  $(p^+, \mathbf{u}^+)$  is the sum of the scattered and radiated fields:

$$(p^+, \mathbf{u}^+) = (p_{sct}, \mathbf{u}_{sct}) + (p_{rad}, \mathbf{u}_{rad}) \quad (3)$$

Figure 1a illustrates the case of an isolated source object, where the field components  $(p^-, \mathbf{u}^-)$  and  $(p^+, \mathbf{u}^+)$  are well defined. They could be determined for example based on measurements across two concentric spherical surfaces that enclose the test object. Figure 1b illustrates the case of measurement with a DLA on a panel section in a cabin. Here, the measurement plane will define the distinction between sources of the incident field and sources of the outward propagating field. The distinction will, however, not be sharp due to the limited angular resolution of a practical array. Figure 2 shows the angular resolution at 2 kHz for the applied 2x8x8 element DLA with 3 cm microphone spacing and 3 cm layer separation. Here, the x-axis shows the incidence angle of a plane wave relative to the array normal, and the curve shows the calculated average pressure on the array centre plane relative to the true pressure of the wave. The SONAH calculation was set up to estimate the field component with sources on one side of the array, and a 20 dB dynamic range was used, [4]. Clearly there is a smooth angular cut-off over an angular interval of approximate size 40°.

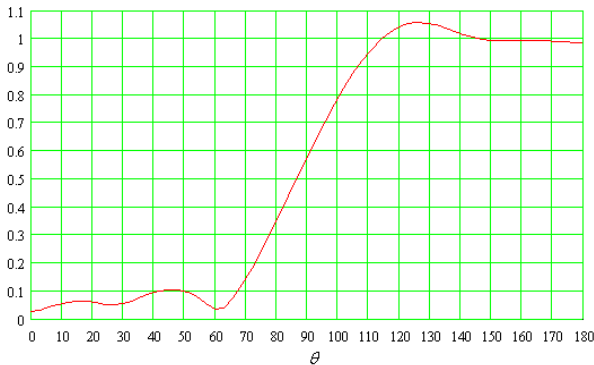


Fig. 2. DLA/SONAH separation of the field component with sources on one side of the array, illustrated through its performance as an angular plane wave filter.

## 2.2 Solution of the scattering problem

If the source surface is locally reacting with a surface admittance  $Y(\mathbf{r})$  that is known at all positions  $\mathbf{r}$  on the surface, then the scattered field  $(p_{sct}, \mathbf{u}_{sct})$  can be completely determined based on the extracted incident field  $(p^-, \mathbf{u}^-)$ . Subtraction of the scattered field from the outward propagating field  $(p^+, \mathbf{u}^+)$  then provides the desired radiated field. The method requires a separate measurement of the surface admittance, which is very sensitive to for example positioning errors, [5].

Provided the incident and radiated fields are mutually incoherent, then Eq. (1) is the basis for a simpler and more robust energy based method. The basic assumption is that we can measure a local absorption coefficient  $\alpha$  at each point  $\mathbf{r}$  on the source surface such that that the normal components  $I^-$  and  $I_{abs}$  of the incident and absorbed intensities are related by:

$$I_{abs}(\mathbf{r}) = \alpha(\mathbf{r})I^-(\mathbf{r}) \quad (4)$$

In general the ratio  $I_{abs}(\mathbf{r})/I^-(\mathbf{r})$  between the two intensities will depend on the form of the incident field. If, however, the coefficient  $\alpha(\mathbf{r})$  is measured with an incident field that is sufficiently similar with the incident field under operational conditions, then Eq. (4) can provide good results.

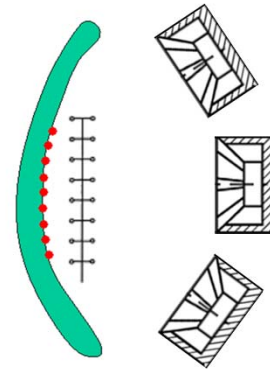


Fig. 3. Cabin panel section with surface calculation points covered by a specific array position. Speakers for measurement of surface properties are shown.

Both methods require a separate set of DLA measurements with artificial speaker excitation. Figure 3 illustrates a set-up with a set of incoherently excited speakers to create an incident field similar to the field incident under for example flight conditions in an aircraft. As mentioned already, the DLA/SONAH measurement can provide the total and incident sound field components on the panel surface. The complex surface admittance is then obtained as the ratio between the normal velocity and the pressure of the total field on the surface. An averaging can here be performed over the principal components. Since in this case the absorbed intensity is equal to the total intensity, then in accordance with Eq. (4) the absorption coefficient is calculated as the ratio between the total and the incident intensities.

For the case of aircraft cabin application, the surface property measurement will typically be performed on the ground, while the operational measurement will be performed during flight. This requires both measurements to provide accurate positioning relative to a common set of calculation points on the panels.

Once the operational measurement has been taken, the total, incident and outgoing fields on the panel surface can be estimated using SONAH. Considering first solution of the scattering problem via the absorption coefficient, the absorbed intensity is estimated using Eq. (4), and the radiated intensity is then obtained using Eq. (1). This method will be called the Energy Method.

The solution of the scattering problem via surface admittance is more complicated, and space does not allow a full derivation here. SONAH provides the pressure and particle velocity of the incident and outgoing field on the

surface. We need to calculate the pressure and particle velocity of the scattered field. For this, the surface admittance provides one set of equations, while SONAH can provide another set of equations, describing the relation between the pressure and particle velocity of the scattered field, [4]. Once the scattered field is obtained, Eq. (3) allows calculation of the radiated field.

### 3 Simulated measurements

In the business jet application addressed in the CREDO project, the primary noise source is the stochastic structural TBL excitation, which creates also a stochastic (“diffuse”) background sound field. Based on purely deterministic Finite Element calculations of a simple vibrating panel structure, a stochastic TBL excitation is simulated. Likewise, a stochastic near-diffuse background field is simulated by superimposing a large number (144) of uncorrelated plane waves. The model of the simple aluminum panel structure is seen in Fig. 4: A plexiglass window is installed in the middle with elastic rubber spacers. The panel is covered with a trim lining with a specified surface impedance, while the window is fully reflective. The coupling between the structure and acoustic domains is one-way, resulting in a locally reacting surface. It should be stressed that this model is not supposed to represent the transmission loss of an aircraft fuselage, but rather to reproduce as closely as possible the kind of measurement challenges that the DLA methodology must cope with. The intensity is mapped across the structure by the 2x8x8 element DLA placed at the positions indicated in Fig. 4 at a distance of 10 mm from the structure. Results from overlapping sections are simply averaged.

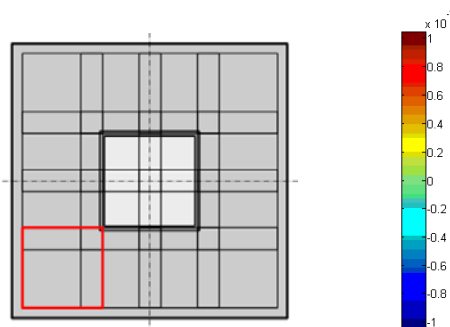


Fig. 4. *Left*: simulated panel structure with window at the centre and 4x4 array positions, one of them shown as red. *Right*: Linear colour scale for intensity plots in Fig. 5 & 6.

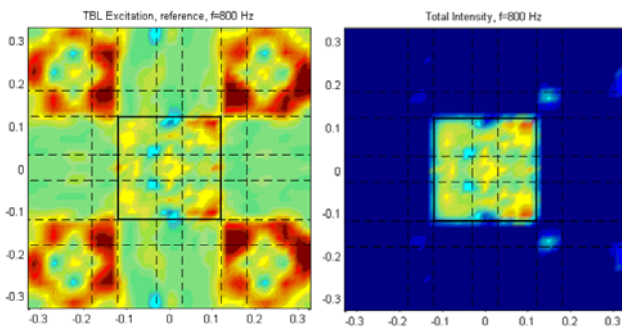


Fig. 5. Intensity maps at 800 Hz directly from FEM model. *Left*: Reference TBL intensity with no diffuse field. *Right*: Total intensity with diffuse field.

The 800 Hz total intensity for a simulation where the ratio between the radiated sound power (from TBL) and the

absorbed sound power (from diffuse field) equals -10 dB is plotted in the right half of Fig. 5. The estimated Entering Intensity (EI) by SONAH is plotted for the two methods in Fig. 6. As observed, both estimates correspond well with the reference intensity in Fig. 5, left, with a slightly better reconstruction for the energy method in this case. Clearly, the extraction of EI works well under ideal conditions, even when the power absorbed from the diffuse field is 10 dB higher than the radiated (entering) power.

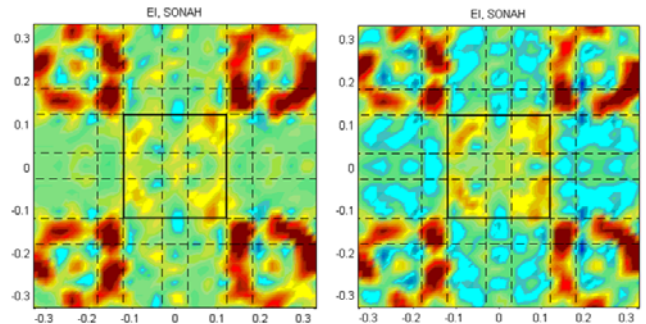


Fig. 6. Entering intensity at 800 Hz. *Left*: Energy method. *Right*: Admittance method.

Considering non-ideal conditions, we focus on differences between the incident field applied for surface properties measurement and the incident field that exists during the operational test. A series of simulated measurements of absorption coefficients and surface admittance were performed with fewer incident plane waves than the 144 waves used in the simulation of the operational measurement. As expected, the admittance method was very insensitive, because the simulated panel is perfectly locally reacting, so only the case with 144 waves will be shown. Figure 7 summarizes the results in terms of the errors in % on the entering sound power for the case of equal radiated power (TBL) and absorbed power (diffuse field) at every frequency between 300 and 800 Hz. This scaling implied the average diffuse field pressure over the microphones to be 5-8 dB higher than the average TBL pressure. The error is relative to the sound power of the reference intensity map in Fig. 5, and it is calculated as:

$$\left[ \frac{(W_{\text{SONAH}} - W_{\text{ref}})}{W_{\text{ref}}} \right] \cdot 100\%$$

The energy method error is shown for the cases of 2, 5, 16 and 144 plane waves used in the measurement of absorption coefficient. Clearly, 2 plane waves are insufficient, while already 5 waves provide low power error. The 5 waves were organized in a way approximated by the loudspeaker set-up in Fig. 8 below: One wave at close to normal incidence and 4 distributed around, far off-axis. The admittance method errors are larger at low frequencies.

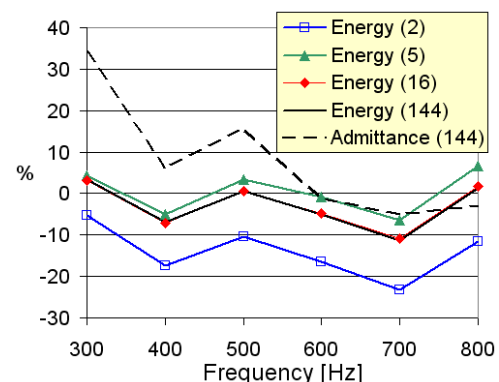


Fig. 7. Sound power error versus number of plane waves used in the simulated measurement of surface properties.

## 4 Measurements

A validation of SONAH has been performed during ground tests at Dassault Aviation acoustic facilities. A panel is fixed between a reverberant and an anechoic room, see Fig. 8. The tested panel is a window panel whose characteristics are close to an aircraft's one. Only one of the two windows is radiating; the other is masked with a heavy viscoelastic patch. The primary structure is exposed to the incident diffuse field in the reverberant room. The window does not radiate directly but through a window shade box that allows the window to be closed with a curtain. The curtain remains open during the tests.



Fig. 8. Set-up with 5 speakers in Transmission Loss facility at Dassault Aviation, France. View from anechoic room.

The power coming from the panel (TL noise) can be measured in anechoic conditions. Five loudspeakers are fixed in front of the panel (see Fig. 8) for measurement of surface absorption coefficient and admittance. The loudspeakers are also used to produce the masking incident field that has to be suppressed in the extraction of the radiated (entering) intensity.

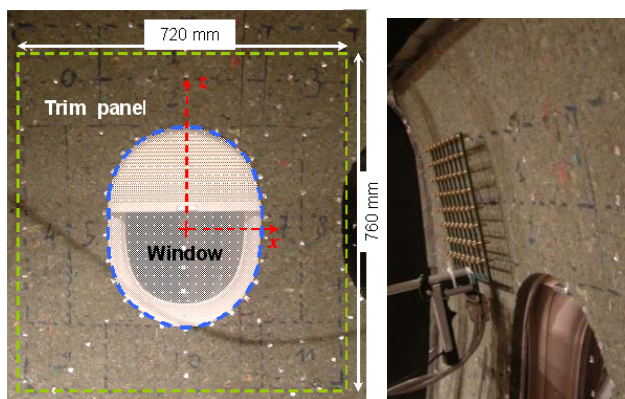


Fig. 9. Window panel. *Left*: measured area around the left window. *Right*: DLA during measurement

The area that will be used for validation and for comparison of results with other methods is shown in the left part of Fig. 9. The area is divided into two sub-areas: the trim panel and the window itself.

Note that as the reverberant room was at the ambient temperature (20°C) and as the spectrum of excitation is not representative of an in-flight excitation, the data presented here are not representative for the in-flight reality.

The following three complementary measured configurations will be used here:

1. Only TL noise: Reference free-field measurement.

2. Only loudspeakers: For determination of surface absorption coefficient and admittance across the area.
3. TL noise and loudspeakers: For extraction of radiated intensity in the presence of background noise.

Each configuration is measured with the DLA and with a normal intensity probe. Beyond these three configurations, a configuration 2a was measured with only the loudspeakers operating, but with reflecting walls set up around the test platform shown in Fig. 8.

Swept measurement of average intensity was performed with a two-microphone sound intensity probe over 12 small areas approximately 5 cm from the panel: 11 on the trim panel and 1 covering the window. Here we will use only area-averaged spectra for the window and for the total surrounding panel.

A set of overlapping array positions were measured across the test area at 1-2 cm distance, see the right part of Fig. 9. The 2x8x8 element DLA was mounted on a xy-robot, but its position and orientation was measured by an InterSense IS-900 system integrated into the handle of the array. Calculations were then performed with SONAH across a mesh at the panel surface.

### Comparison of total intensities

The estimation of total intensity by the DLA can be compared to the one measured with the classical probe. Figure 10 shows the area averaged intensities for configuration 3 (TL noise and loudspeakers) in 1/3-octave bands. The two techniques give results that are typically within 1.0 dB. It should be noted that the DLA intensities are on the panel surface, while the intensity probe measurements were taken approximately 5 cm from the panels. For the classical probe measurement this means that some of the power from the window will actually be measured over the panel.

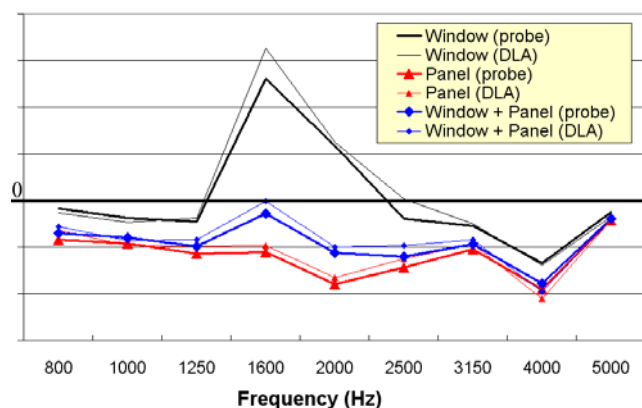


Fig. 10. Area averaged total intensity 1/3-octave spectra. The y-axis shows linear intensity ( $\text{W}/\text{m}^2$ ).

### Estimation of absorption coefficient

For the measurement of the absorption coefficient, the 5 loudspeaker shown in Fig. 8 were excited by incoherent broadband noise of equal level. Figure 11 shows a comparison of the absorption coefficient spectrum of the homogeneous panel surface obtained from the DLA measurement and from a normal incidence measurement on a test sample in a plane wave tube. The DLA result is given for a single calculation position and averaged over a small area. The agreement is good, keeping in mind that the tube measurement is for normal incidence only, while the DLA measurement has incident waves from many directions.

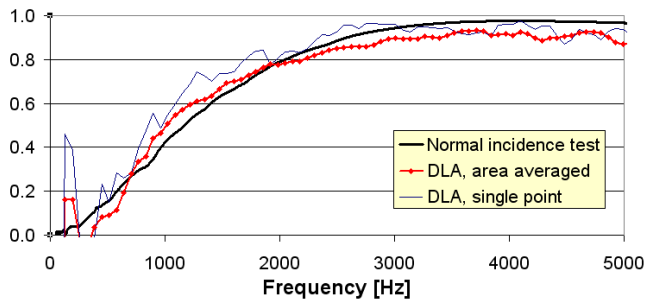


Fig. 11. Absorption coefficient spectra of the panel surface from an impedance tube and from the DLA measurement.

### Estimation of radiated intensity

Figure 12 shows the contour maps of total sound intensity on the panel around the left window for a single octave band calculated by SONAH. The two plots represent the configurations 1) only TL noise and 3) TL noise and loudspeaker noise. Clearly, in configuration 3 the absorbed power is much stronger than the radiated power.

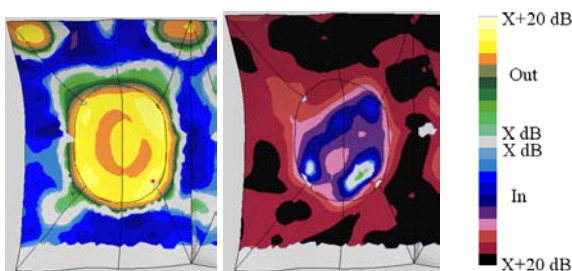


Fig. 12. SONAH total intensity maps.

Left: TL noise. Middle: TL noise and loudspeakers

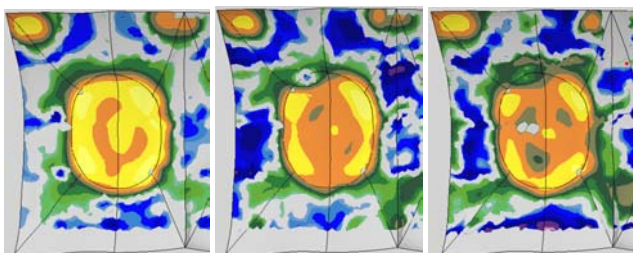


Fig. 13. SONAH EI maps based on energy method.

Left: TL noise. Middle: TL noise and loudspeakers.

Right: TL noise and loudspeakers, surface test 2a.

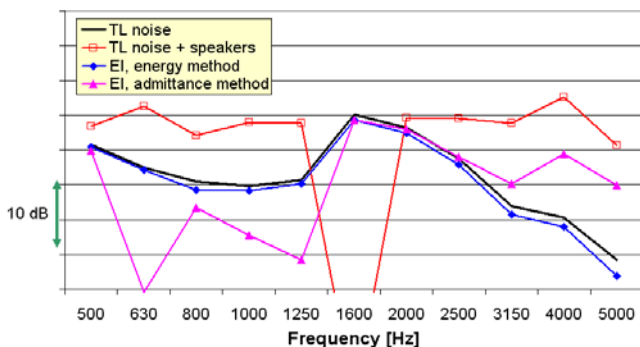


Fig. 14. 1/3-octave sound power spectra for the “window + panel” area defined in relation to Fig. 9, which is the area mapped in Fig. 12 & 13 minus an upper strip.

Figure 13 shows 3 EI maps obtained using the energy method. For the 2 leftmost maps, the absorption coefficient has been taken from the configuration 2 measurement, while configuration 2a has been used in the third. The leftmost map shows EI obtained from the TL noise only measurement. Some of the negative intensity has been removed, being treated partly as being due to an incident field from neighbouring areas. The middle map shows EI

extracted from the measurement with both TL noise and loudspeaker noise. Even in the presence of the much stronger loudspeakers noise the left-most TL-noise EI map is well reconstructed. So far, however, the incident fields during the operational and surface measurements have been almost identical, which makes the suppression easier. The two incident fields were therefore made different by adding reflecting walls in the surface property measurement (2a), but the rightmost map shows still good extraction of the EI.

Figure 14 shows how well the energy method reconstructs the 1/3-octave sound power spectrum, while the admittance method exhibits some outliers.

## 5 Conclusions

Two methods for measurement of radiated intensity based on array measurements and SONAH calculations have been described. The methods have been validated and compared through simulated measurements on a model of an aircraft panel section and through a set of actual measurements on a panel section in a transmission loss facility. The experimental validation gave the following results: The total intensity is very well measured; the in-situ measurement of absorption coefficient gives realistic results; the extraction of entering intensity is good even with high levels of back-ground noise (>15 dB) and over a wide frequency range (up to 5700 Hz). The SONAH mapping further provides high spatial resolution. A planned set of experiments will focus on the sensitivity of the methods to differences between the incident fields during the operational and the surface properties measurement.

## Acknowledgments

This research has been carried out within the CREDO project, funded by the European Commission in the 6<sup>o</sup> Framework Programme (Thematic Priority: Aeronautics and Space, AST5-CT-2006-030814).

## References

- [1] P. Hardy, D. Trentin, L. Jézéquel and M. N. Ichchou, “Identification of noise sources in an in-flight aircraft by means of local energy method”, Proceedings of Euronoise 2006.
- [2] J. Hald, “STSF - a unique technique for scan-based Near-field Acoustical Holography without restrictions on coherence”, B&K Technical Review, No. 1, 1989.
- [3] J. Hald, “Patch holography in cabin environments using a two-layer handheld array with an extended SONAH algorithm”, Proceedings of Euronoise 2006.
- [4] J. Hald and J. Mørkholt, “Methods to estimate the Entering Intensity and their implementation using SONAH”, Report DWP2.3 from the European project CREDO, 2007.
- [5] J. D. Alvarez and F. Jacobsen, “In-situ measurements of the complex acoustic impedance of porous materials”, Proceedings of Inter-Noise 2007.